Core/shell $CoFe_2O_4$/Fe_3O_4 nanoparticles: effects of hard/soft magnetic weight fraction on structure, particle size and magnetic properties

Tran Thi Viet Nga[†], **Chu Manh Hung and Truong Tien Hoang Duong**

International Training Institute for Materials Science,
Hanoi University of Science and Technology,
No. 1 Dai Co Viet road, Hanoi, Vietnam

E-mail: [†]vietnga@itims.edu.vn

Abstract. *$CoFe_2O_4$/Fe_3O_4 nanocomposite particles were synthesized by using co-precipitation combined with hydrothermal methods. The phase composition, surface morphology and magnetic properties of the nanocomposites were investigated using X- ray diffraction, scanning electron microscopy and vibrating sample magnetometer. Findings show that the samples comprise two phases, and Fe_3O_4 particles are coated on the surface of $CoFe_2O_4$ particles. The average particle size of $CoFe_2O_4$ was ditrisbuted in the range of $50 - 100$ nm. While the particle of Fe_3O_4 displayed a spherical shape and particle size distributed from $10 - 20$ nm. The MS of $CoFe_2O_4@Fe_3O_4$ core–shell particles increase with the decrease in the mass ratio of hard to soft ferrites. The structure, magnetic properties and the degree of exchange coupling between the magnetic phases were investigated.*

Keywords: nanocomposite; core- shell; exchange- spring.

Classification numbers: 75.75.Fk; 75.70.Kw.

1. Introduction

Nanocomposite magnetic materials that consist of hard and soft magnetic phases have recently attracted a great attention of researchers over the world because of various potential applications such as magnetic recording media, microwave devices, permanent magnets and biomedical [1–5]. By combining high saturation magnetization of soft magnetic phase and high

coercivity of hard magnetic phase, exchange - coupled nanocomposite materials can possess enhanced magnetic properties compared with the individual soft and hard material. In addition to size, shape and weight ratio between two phases, the magnetic properties of nanocomposite magnetic materials depend on their architectures. There are three main architectures: layered structure, soft inclusion in hard and hard inclusion in soft [6] (Fig. 1). In "layered structure", the magnetic phases only have an exchange coupled at the interface. The coercivity is predicted from the micromagnetic energy equations varies as $1/L_2$ as a function of the soft layer thickness L. The hysteresis loops of the nanocomposite exhibited a typical "exchange- spring", suggesting the weak interaction between the hard and soft phases. For the "soft inclusion in hard", when the distance between the soft inclusion is small, the magnetization mode tunnel through the hard region. So the exchange interaction reduces the coercivity if the width of the hard magnetic phase is less than the domain wall width l_w (Fig. 1b). And the "hard inclusion in soft", from the random anisotropy model, which assumes an assembly of randomly oriented and ferromagnetically coupled grains, one can determine the mean anisotropy of the system with a volume V [6]. If the grain size (D) exceeds exchange length, magnetocrystalline anisotropy is determined by the full magneto- crystalline anisotropy K_1. The coercivity is maximum when $D \sim l_{ex}$ (l_{ex} is called the exchange length). And the grain exceeds domain wall width, the coercivity decreases proportional to $1/D$.
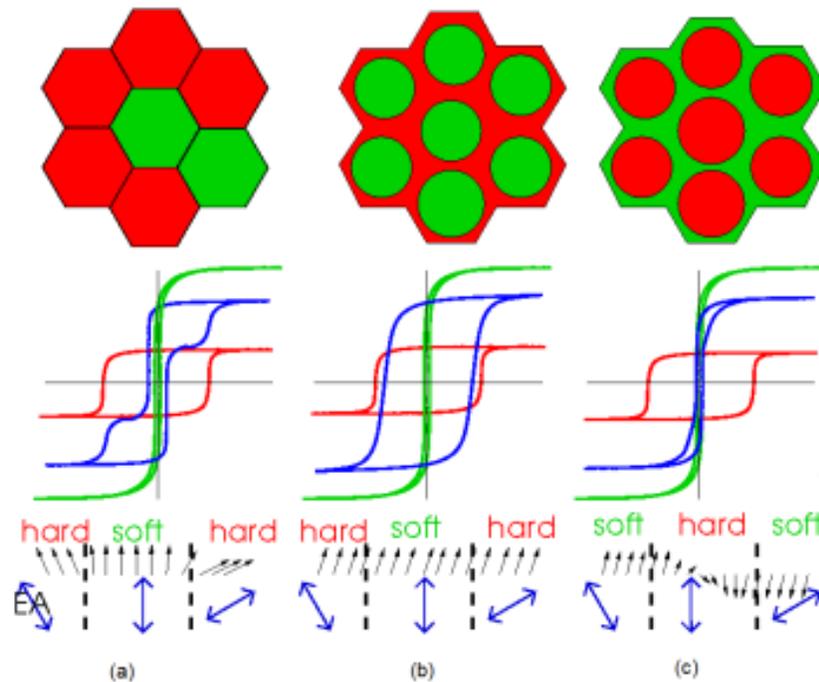
Fig. 1. Schematic for exchange spring hard- soft nano- structures and its corresponding magnetic bahavior: (a) Layer structure, (b) Soft inclusion in Hard and (c) Hard inclusion in Soft [6].

Nanocomposites composed of hard and soft ferrite have been synthesized with good exchange coupled between two phases. Hard/soft composite powders such as CoFe$_2$O$_4$/CoFe [7],

$CoFe_2O_4$- Fe_3O_4 [8], $MnFe_2O_4$@$CoFe_2O_4$ [9], $CoFe_2O_4$@ Fe_3O_4 and Fe_3O_4@ $CoFe_2O_4$ [9], $BaFe12O19$@Fe_3O_4 [10], $SrFe_{12}O_{19}$@Fe_3O_4 [11]... were prepared and the reports showed excellent exchange coupling and enhanced saturation magnetization while coercivity decrease with increase soft magnetic phase. According to the data of the review papers [5, 12], for core-shell magnetic nanoparticles, the soft and hard phases will reverse if the size of the soft phase is sufficiently large. And the size of the soft phase is reduced to about twice the domain wall width of the hard phase. In addition, when the size of the magnetic materials is down to the nanoscale, the magnetic properties do not only depend on the difference in magnetic parameters between the core and shell materials but also the presence of the dipolar and exchange-coupled interactions that affect the spin reversal processes [13].

In this study, we fabricated nanocomposites consisting of $CoFe_2O_4$ as the hard phase and Fe_3O_4 as the soft phase synthesized co-precipitation combined with hydrothermal method. The weight ratio of $CoFe_2O_4$/ Fe_3O_4 was varied from 1/2, 1/1 and 2/1. The magnetic properties, architecture and the degree of exchange coupling between two phases were discussed.

2. Experiment

Details of synthesis samples, iron (III) chloride nonahydrate (97% $FeCl_3 \cdot 9H_2O$, Sigma Aldrich), cobalt (II) chloride nonahydrate (98% $CoCl_2 \cdot 6H_2O$, Sigma Aldrich), iron (II) chloride (99% $FeCl_2$, Sigma Aldrich), NHl_3 solution, ethylene glycol $HOCH_2CH_2OH$ (99% EG, Sigma Aldrich) and ure NH_2CONH_2 (99%, Sigma Aldrich) were used as starting reagents. All stages of synthesis were carried out in a three- neck flask.

Synthesis of $CoFe_2O_4$ and Fe_3O_4 nanoparticles

$CoFe_2O_4$ nanoparticles were synthesized by coprecipitating chlorides of Co2+ and Fe3+ cations with molar ratio of 2:1 in aqueous solution with pH = 7. Fe_3O_4 nanoparticles were also synthesized by coprecipitating chlorides of Fe3+ and Fe2+ cations with molar ratio of 2:1 in nitrogen atmosphere. NHl_3 solution was used as the reactive agent. The obtained articles were washed many times with distilled water followed by acetone rinse and dry at room temperature.

Synthesis of $CoFe_2O_4$@Fe_3O_4 nanocomposite particles

$CoFe_2O_4$/Fe_3O_4 nanocomposite powder was synthesized using the $CoFe_2O_4$ and Fe_3O_4 nanoparticles obtained previously. $CoFe_2O_4$ and Fe_3O_4 nanoparticles were mixed mechanically with mass ratios $CoFe_2O_4$/Fe_3O_4 of 1/ 1. The sample was labeled as Mix11.

The series of $CoFe_2O_4$@Fe_3O_4 nanocomposite particles with core-shell structure were synthesized by co-precipitation method combined with hydrothermal method. Total of 0.5 g of $CoFe_2O_4$ powders was dissolved in 100 ml ethylene glycol $C_2H_6O_2$ ultrasonically for 2 hours. This solution was stirred at 1000 rpm and 40˚C (mixture A). Then, $FeCl_3 \cdot 9H_2O$ (with mass 0.25, 0.5 and and 1 g) and 2.7 g urea NH_2CONH_2 were added to the mixture A and stirred for 30 min (mixture B). Then, we transferred the mixture B in a Teflon lined stainless-steel autoclave with a 100 ml capacity at 180˚C and stored for 24 h in an oven. The autoclave was air cooled to room temperature. Finally, the precipitated products were washed with deionized water and then dried at 80˚C for 24 h in vacuum. The samples of $CoFe_2O_4$@Fe_3O_4 core- shell nanocomposites with the mass ratio $CoFe_2O_4$/Fe_3O_4 of 2/1, 1/1 and 1/2 were labeled as CF21, CF11 and CF12.

3. Characterization

The crystal structure and phases of the obtained samples were identified via X-ray powder diffraction (XRD) using a Siemens D5000 diffractometer (CuK$_\alpha$ radiation, $\lambda = 1.5405$ Å). The morphology and the particle size were observed via scanning electron microscopy (SEM, JEOL-JSM 7600F). The magnetic properties were measured using a vibrating sample magnetometer (VSM, Lakeshore 7410) with applied magnetic fields of up to 15 kOe.

4. Results and disscution
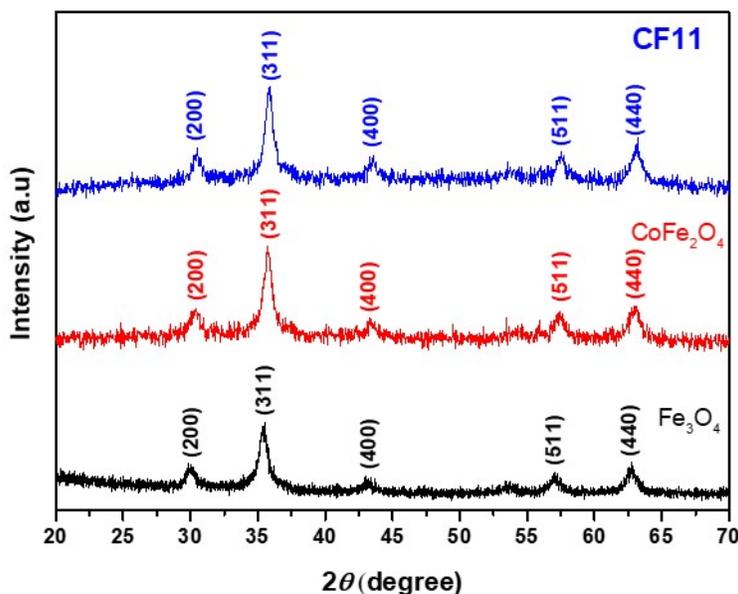
Fig. 2. XRD patterns of shell Fe$_3$O$_4$, core CoFe$_2$O$_4$ and CoFe$_2$O$_4$@Fe$_3$O$_4$ (CF11) core-shell nanocomposite sample.

XRD patterns of shell Fe$_3$O$_4$, core CoFe$_2$O$_4$ and core- shell CoFe$_2$O$_4$@Fe$_3$O$_4$ (CF11) nanocomposites (Fig. 2) show the typical reflections of a spinel phase. All the observed peaks of samples are close to the characteristic peaks in the JCPDS cards of Fe$_3$O$_4$ (No. 19-0629) or CoFe$_2$O$_4$ (No. 22-1086). We can not distinguish the characteristic peaks of Fe$_3$O$_4$ and CoFe$_2$O$_4$ due to their very close positions [14], and no extra peak within the resolution of XRD technique is detected.

Figure 3 shows the SEM images of CoFe$_2$O$_4$, Fe$_3$O$_4$ and Mix11 samples. It clearly shows that the Fe$_3$O$_4$ nanoparticles exhibited spherical morphology with a mean particle size of 20 nm (Fig. 3b). Whereas CoFe$_2$O$_4$ particles exhibited hexagonal- like morphology and the average particle size were ditrisbuted in the range of 50 – 100 nm (fig 3a). The Mix11 nanocomposite sample composed two type of grains: Fe$_3$O$_4$ with smaller size and CoFe$_2$O$_4$ with lager size. The particles are not well distributed and are agglomerated (Fig. 3c). This may be due to the magnetic interactions between them [15]. Therefore, this mechanical mixing method is an inadequate method

for obtaining exchange-spring magnets because of non-homogeneously distributed soft and hard magnetic phases.
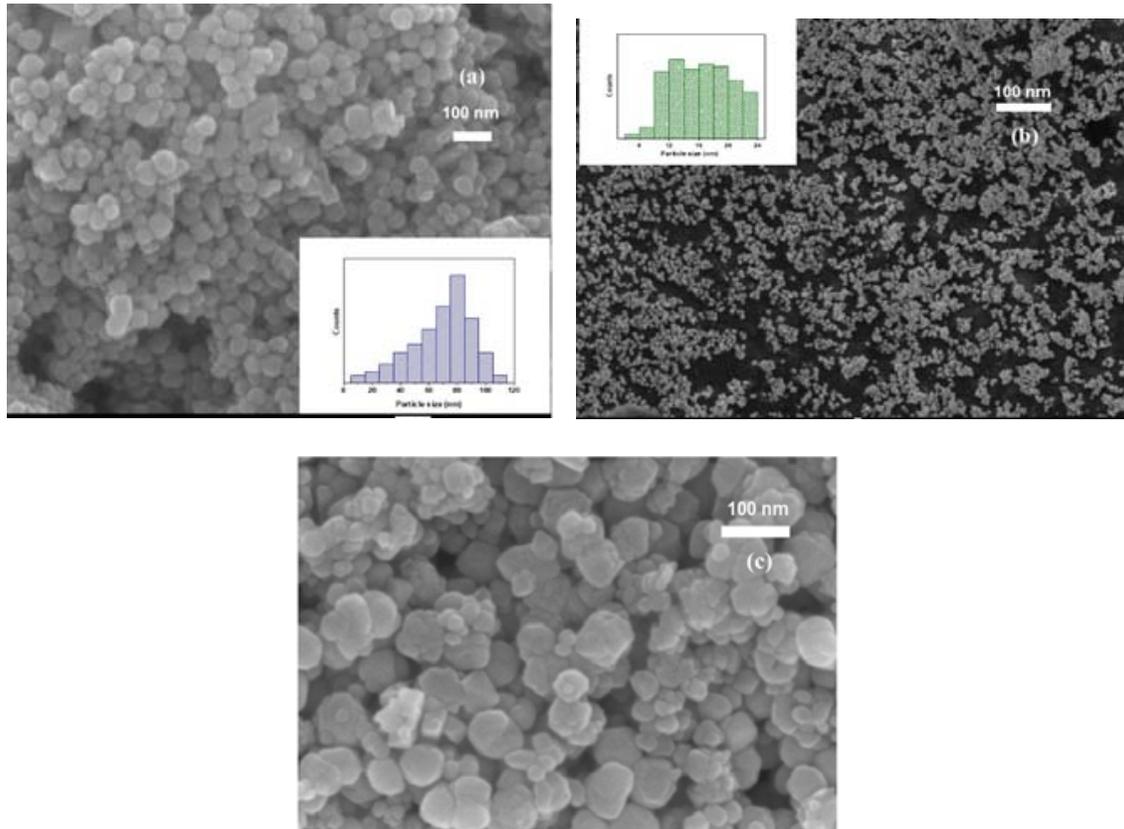
Fig. 3. SEM micrographs of core $CoFe_2O_4$ (a), shell Fe_3O_4 (b) and Mix11 (c).

The SEM images of CF21, CF11 and CF12 particles are illustrated in Fig. 4. It could be seen that CF21, CF11 and CF12 samples consisted of numerous highly uniform spheres with a rough surface. The average particle size increases from 70 to 120 nm when the ratio $CoFe_2O_4/Fe_3O_4$ varied from 2/1 to 1/2. The sphere particles were constructed with numerous sphere shaped primary particles in a diameter range from 10- 20 nm. Thus, we can conclude that the Fe_3O_4 nanopartilces have been successfully dispersed on the $CoFe_2O_4$ particles surface. Such observation was also perceived in the synthesis of $SrFe_{12}O_{19}$- $CoFe_2O_4$ [16], $SrFe_{12}O_{19}@Fe_3O_4$ [11], $CoFe_2O_4$-Fe_3O_4 [17] core- shell nanocomposites. With the ratio of $CoFe_2O_4/Fe_3O_4$ of 1/2, the Fe_3O_4 microspheres more deposited on the $CoFe_2O_4$ particles surface and the obtained core-shell nanocomposites have diameter distribution range of 100- 120 nm. This phenomenon can be understood via Fe_3O_4 nanoparticles occupy a large percentage of the volume and thus are able to cover the specific surface area of $CoFe_2O_4$ significantly. These results agreed with those reported by C. Borgohain and J. P. Borah [17]. For $CoFe_2O_4$- Fe_3O_4 nanocomposites were fabricated through the combination sonochemical and reverse co-precipitation method.
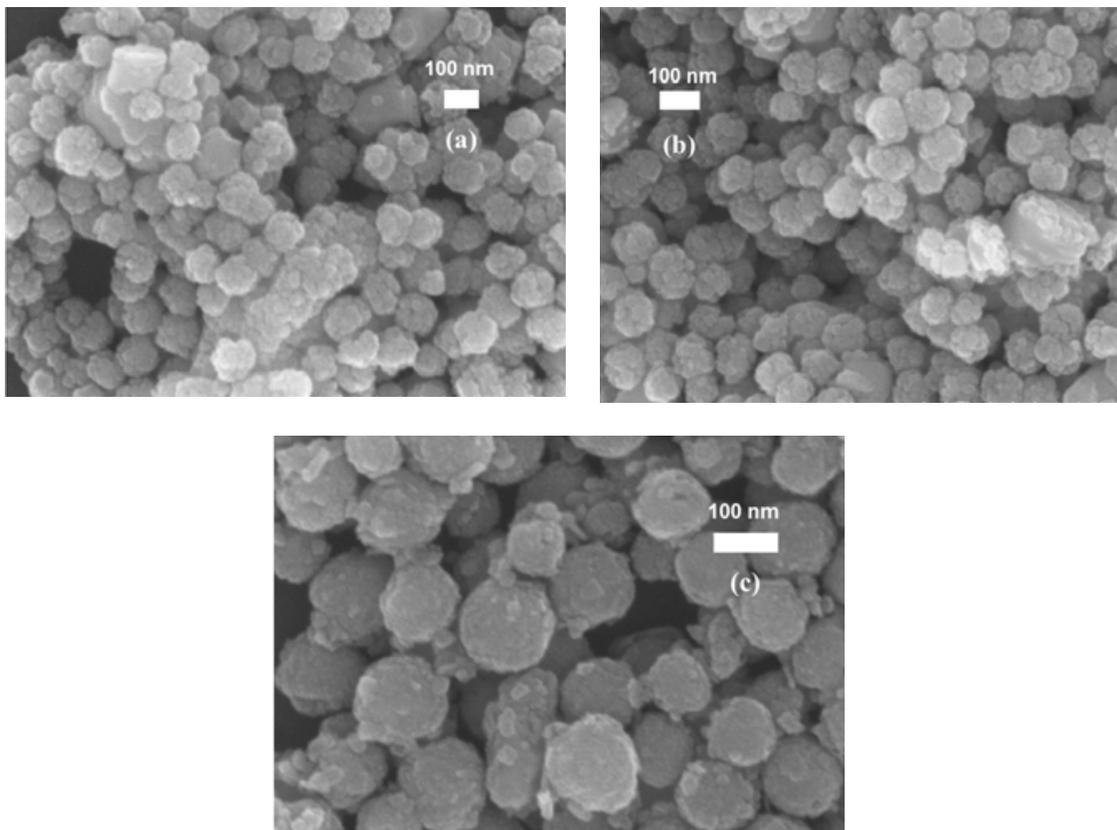
Fig. 4. SEM micrographs of CF21 (a), CF11 (b) and CF12 (c) core- shell nanocomposite sample.

The magnetic behavior of samples was evaluated by the magnetization curves measured at room temperature and are shown in Figs. 5 and 6. The Fig. 5 depicts the hysteresis loops of CoFe$_2$O$_4$ and Fe$_3$O$_4$ nanoparticles. The CoFe$_2$O$_4$ nanoparticles exhibit a magnetically hard behavior with the coercivity (HC) of 1.7 kOe and saturation magnetization (MS) of 55 emu/g. While, the hysteresis loop of Fe$_3$O$_4$ nanoparticles shows a magnetically soft behavior with HC of 0.5 kOe and MS of 70 emu/g. It has been reported that Fe$_3$O$_4$ and CoFe$_2$O$_4$ are spinel ferrites which possess saturation magnetization 94 emu/g [18] and 80 emu/g [5], respectively. The lower magnetization compared to their bulk may be due to the particle size effect [19].

The hysteresis loops of Mix11 samples showed a typical "exchange- spring" [5] (Fig. 6a). That is, they showed the presence of two phases in the hysteresis loop instead of a single phase. According to Chakka *et al.* [20], the hard and soft magnetic phases are switching individually and magnetization includes two step reversal processes due to the in- complete exchange- coupling and this sample may be represented as a "layered structure" [6]. For this structure, the soft phase switches easily and the HC of the nanocomposite sample decreases compared with that of the hard phase. In addition, the non- homogeneous distribution of two phases can be a reason for
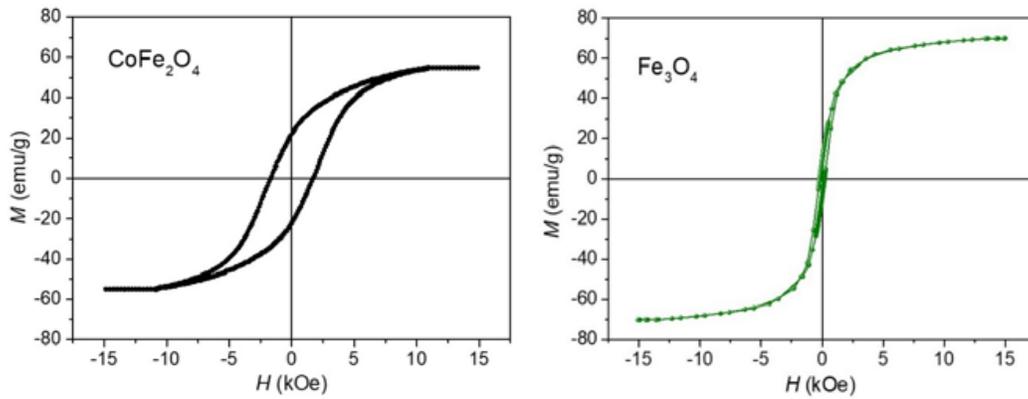
Fig. 5. Hysteresis loops of core CoFe$_2$O$_4$ and shell Fe$_3$O$_4$.
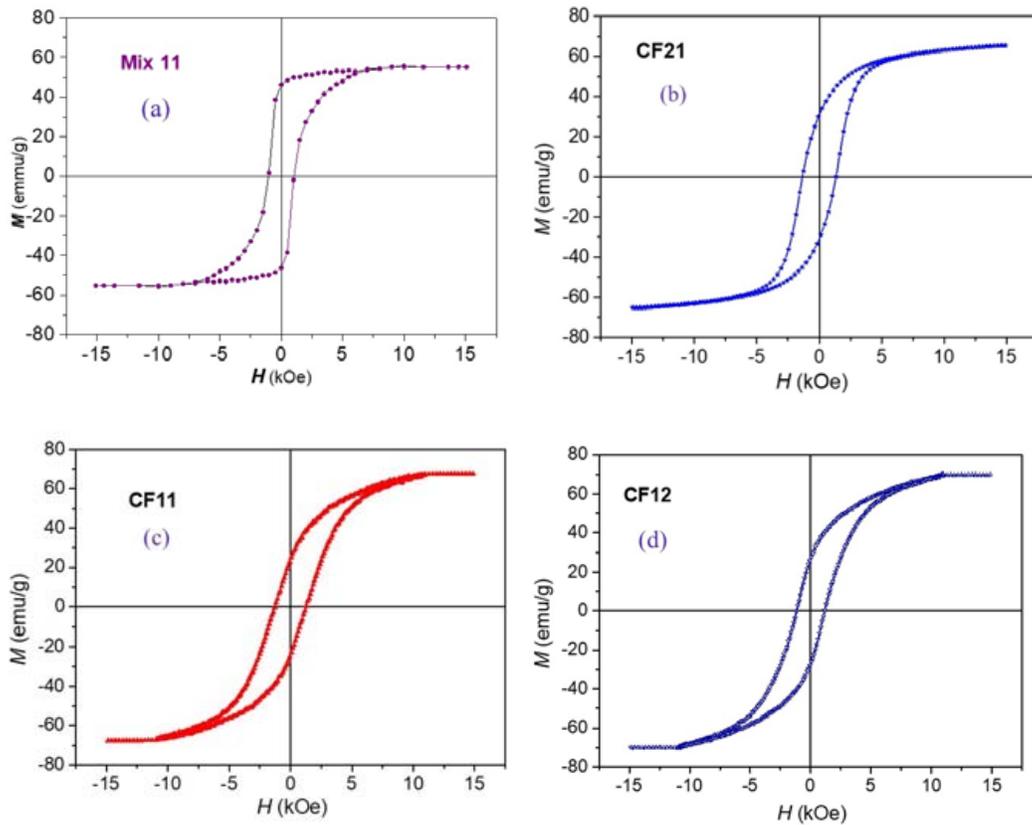
Fig. 6. Hysteresis loops of Mix11 and CF21, CF11 and CF12 core- shell nanocomposite sample.

the decreasing of HC and MS compared CoFe$_2$O$_4$ core (Fig. 3c). HC and MS of Mix11 sample reach 1.02 kOe and 53.17 emu/g. While the hysteresis loops of the nanocomposite samples

(CF21, CF11 and CF12) show single- step hysteresis loops suggesting the hard magnetic phase and the soft magnetic phase are exchange coupled to each other [21]. From Fig. 4, we can observe that nanocomposite particles were composed of Fe$_3$O$_4$ soft nanoparticles cover on the surface of CoFe$_2$O$_4$ hard nanoparticles. So they may be represented as a "hard inclusion in soft" structure [6]. According to Alberto Lospez- Ortega *et al.* [5], for the thin soft thickness, there is a critical thickness below which the soft phase is rigidly coupled to the hard phase and two phases reverse at the same nucleation field, resulting in a rectangular hysteresis loop (Fig. 1c). The MS of the nanocomposite increases from 65.21 to 69.75 emu/g with increase in Fe$_3$O$_4$ weight. The MS of CF12 sample is larger about 27% than that of CoFe$_2$O$_4$ core. This result was mainly attributed to the MS of Fe$_3$O$_4$ is higher than that of CoFe$_2$O$_4$ and the development of particle size with increase in Fe$_3$O$_4$ weight [11, 23].

The exchange coupling in the nanocomposites can be further clarified by the switching field distribution curves dM/dH [12, 22, 23]. In the case of effective exchange coupling, there exists only one peak, indicating that one step of magnetic reversal was completed in the nanocomposite samples. If the magnetic phases are decoupled or have weak coupling, two different peaks will be observed in low and high coercivity regions. A low- intensity peak which appears at the high field of the switching field distribution curves shows a relatively high degree of exchange coupling. In this study, the CF sample displayed a single peak at the high field and no significant peak formed at the low field, indicating that magnetization of two magnetic phases switches at the same magnetic field. And we can observe the peak intensity decrease with the decrease in the mass ratio of hard to soft ferrites (Fig. 7), it indicates that the improvement of the exchange coupling with the increase in Fe$_3$O$_4$ weight.
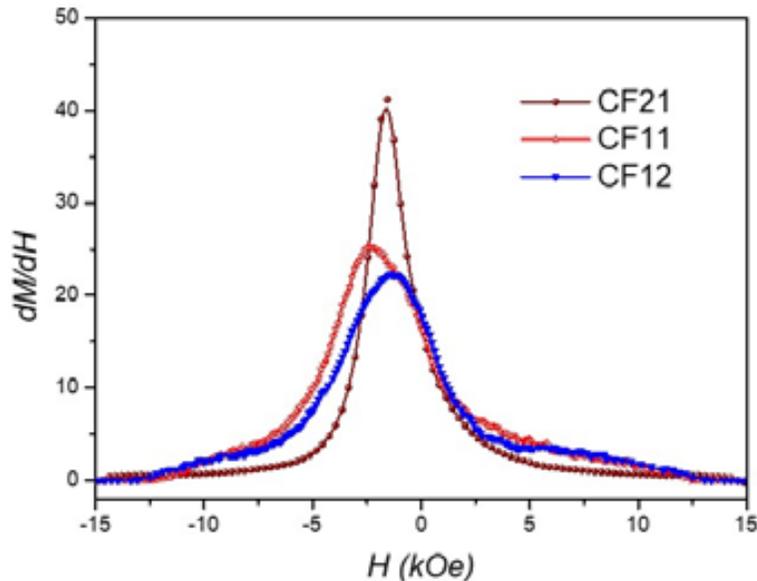
Fig. 7. Swithching field distribution curves of CF21, CF11 and CF12.

The HC decrease from 1.38 kOe to 1.14 kOe with an increase in Fe_3O_4 content. When increasing the weight of Fe_3O_4, the core $CoFe_2O_4$ may be covered a thick layer by the Fe_3O_4 particles. Thus, the magnetic properties of nanocomposite samples exhibited the soft magnetic properties of Fe_3O_4. Otherwise, the particle size of nanocomposite sample (D) increases with decreasing the ratio of $CoFe_2O_4/Fe_3O_4$ (see Fig. 4). Hence, the coercivity decreases proportional to 1/D. These results were in agreement with those reported by Fan Yi [2]. In which, the composite ceramic of $CoFe_2O_4/ Fe_3O_4$ with different core-shell ratios were synthesized by Spark Plasma Sintering at a sintering temperature of 500˚C.

Table 1. Average particles size $< D >$, saturation magnetization MS, coercivity HC of samples.

Sample	$< D >$ (nm)	M_S (emu/g)	H_C (kOe)
$CoFe_2O_4$	80	55	1.7
Fe_3O_4	20	70	0.5
Mix11	-	53.17	1.02
CF21	100	65.21	1.38
CF11	110	67.59	1.26
CF12	130	69.75	1.14

5. Conclusion

The $CoFe_2O_4@ Fe_3O_4$ nanocomposite with core- shell structure were prepared successfully by combining co-precipitation method and hydrothermal method. The SEM micrographs of the CF samples showed that Fe_3O_4 nanoparticles were coated on the surface of the $CoFe_2O_4$ particles. And the average particle size increases from 70 to 120 nm when the ratio $CoFe_2O_4/Fe_3O_4$ varied from 2/1 to 1/2. The degree of exchange coupling between the magnetic phases was studied using the switching field distribution curves dM/dH. The result shows that the improvement of the exchange coupling with the decrease in the mass ratio of hard to soft ferrites. The MS of the nanocomposite increases from 65.21 to 69.75 emu/g and the HC decrease from 1.38 kOe to 1.14 kOe with an increase in Fe_3O_4 weight.

Acknowledgment

Conflict of interest

The authors declare that they have no competing financial interests.

References

[1] D. A. Allwood, G. Xiong, M. D. Cooke, C. C. Faulkner, D. Atkinson, N. Vernier, *Submicrometer ferromagnetic NOT gate and shift register*, *Science* **296** (2006) 2003.

[2] F. Yi, *Magnetic properties of hard (CoFe$_2$O$_4$)-soft (Fe$_3$O$_4$) composite ceramics*, *Ceram. Int.* **40** (2014) 7837.

[3] J. Jin, X. Sun, M. Wang, Z. L. Ding and Y. Q. Ma, *The magnetization reversal in CoFe$_2$O$_4$/CoFe$_2$ granular systems*, *J. Nanoparticle Res.* **18** (2016) 2.

[4] K. Simeonidis, C. Martinez-Boubeta, D. Serantes, S. Ruta, O. Chubykalo-Fesenko, R. Chantrell, J. Oró-Solé, Ll. Balcells, A.S. Kamzin, R.A. Nazipov, A. Makridis and M. Angelakeris, *Controlling magnetization reversal and hyperthermia efficiency in core-shell iron-iron oxide magnetic nanoparticles by tuning the interphase coupling*, *ACS Appl. Nano Mater.* **3** (2020) 4465.

[5] A. López-Ortega, M. Estrader, G. Salazar-Alvarez, A. G. Roca and J. Nogués, *Applications of exchange coupled bi-magnetic hard/soft and soft/hard magnetic core/shell nanoparticles*, *Phys. Rep.* **553** (2015) 1.

[6] Renuka Tayade, *Theoretical and experimental contribution to the study of exchange-spring magnets*, Materials Science [cond-mat.mtrl-sci]. École normale supérieure de Cachan - ENS Cachan, 2014.

[7] G. Du and S. Wang, *Synthesis of magnetically exchange coupled CoFe$_2$O$_4$/CoFe$_2$ core/shell composite particles through spray pyrolysis*, *J. Alloys. Comp.* **708** (2017) 600.

[8] M. Abbas, M. N. Islam, B. Parvatheeswara Rao, K. E. Abou Aitah and C. Kim, *Facile approach for synthesis of high moment Fe/ferrite and FeCo/ferrite core/shell nanostructures*, *Mater. Lett.* **139** (2015) 161.

[9] J. H. Lee, J. Jang, J. Choi, S. H. Moon, S. Noh, J. Kim, J. G. Kim, L. S. Kim, K. I. Park and J. Cheon, *Exchange-coupled magnetic nanoparticles for efficient heat induction*, *Nat. Nanotechnol.* **6** (2011) 418.

[10] H. Xianghui and C. Zhenhua, Preparation and characteriza- nanocomposites, 51 (2006) 2529.

[11] T. T. V. Nga and N. T. Lan, *Fabrication and exchange-spring properties of SrFe$_{12}$O$_{19}$@ Fe$_3$O$_4$ nanocomposites with core-shell structure*, *Mater. Chem. Phys.* **251** (2020) 123084.

[12] F. Liu, Y. Hou and S. Gao, *Exchange-coupled nanocomposites: Chemical synthesis, characterization and applications*, *Chem. Soc. Rev.* **43** (2014) 8098.

[13] A. M. Belemuk and S. T. Chui, *Finite temperature performance of hard-soft composite nanomagnets and its dependence on geometry structure of composites*, *J. Appl. Phys.* **113** (2013) 4788703.

[14] J. Robles, R. Das, M. Glassell, M. H. Phan and H. Srikanth, *Exchange-coupled Fe$_3$O$_4$/CoFe$_2$O$_4$ nanoparticles for advanced magnetic hyperthermia*, *AIP Adv.* **8** (2018) 007249.

[15] Shabab Torkian, Ali Ghasemi and Reza Shoja Razavi, *Magnetic properties of hard-soft SrFe$_{10}$Al$_2$O$_{19}$/Co$_{0.8}$Ni$_{0.2}$Fe$_2$O$_4$ ferrite synthesized by one-pot sol–gel auto-combustion*, *J. Magn. Magn. Mater.* **416** (2016) 408.

[16] A. Xia, S. Ren, J. Lin, Yue Ma, C. Xu, J. Li, C. Jin, X. Liu, *Magnetic properties of sintered SrFe$_{12}$O$_{19}$-CoFe$_2$O$_4$ nanocomposites with exchange coupling*, *J. Alloys. Comp.* **653** (2015) 108.

[17] C. Borgohain and J. P. Borah, *CoFe$_2$O$_4$-Fe$_3$O$_4$ bimagnetic heterostructure: A versatile core-shell nanoparticle with magnetically recoverable photocatalytic and self heating properties*, *Mater. Res. Express.* **7** (2020) 2053.

[18] A. S. Teja and P. Y. Koh, *Synthesis, properties and applications of magnetic iron oxide nanoparticles*, *Prog. Cryst. Growth. Charact. Mater.* **55** (2009) 22.

[19] R. H. Kodama and A. E. Berkowitz, *Atomic-scale magnetic modeling of oxide nanoparticles*, *Phys. Rev. B* **59** (1999) 6321.

[20] V. M. Chakka, Z. S. Shan and J. P. Liu, *Effect of coupling strength on magnetic properties of exchange spring magnets*, *J. Appl. Phys.* **94** (2003) 6673.

[21] K. P. Remya, D. Prabhu, S. Amirthapandian, C. Viswanathan and N. Ponpandian, *Exchange spring magnetic behavior in BaFe12O19/Fe$_3$O$_4$ nanocomposites*, *J. Magn. Magn. Mater.* **406** (2016) 233.

[22] J. E. Davies, O. Hellwig, E. Fullerton, J. S. Jiang, S. D. Bader, G. T. Zimányi and K. Liu, *Anisotropy dependence of irreversible switching in Fe/SmCo and FeNi/FePt exchange spring magnet films*, *Appl. Phys. Lett.* **86** (2005) 1.

[23] J. Liang, X. Wu, W. Wu, L. Chen, Y. Huang and Y. Huang, *Improved magnetic properties of Sr$_{0.93}$Sm$_{0.10}$Fe$_{11.97}$O$_{19}$/Fe$_3$O$_4$ composite powders by substitution of Sm and magnetic exchange coupling effect*, *J. Mater. Sci.* **31** (2020) 20400.